Available online at www.sciencedirect.com

SciVerse ScienceDirect

Ceramics International 38 (2012) 5015–5022

CERAMICS INTERNATIONAL

www.elsevier.com/locate/ceramint

The fabrication and mechanical properties of SiC/ZrB_2 laminated ceramic composite prepared by spark plasma sintering

Hailong Wang [a,*], Bingbing Fan [a], Lun Feng [a], Deliang Chen [a], Hongxia Lu [a], Hongliang Xu [a], Chang-An Wang [b], Rui Zhang [a,c]

[a] School of Materials Science and Engineering, Zhengzhou University, Zhengzhou 450001, China

[b] State Key Laboratory of New Ceramics and Fine Processing, Department of Materials Science and Engineering, Tsinghua University, Beijing 100084, China

[c] Zhengzhou Institute of Aeronautical Industry Management, Zhengzhou 450015, China

Received 6 September 2011; received in revised form 28 February 2012; accepted 29 February 2012
Available online 7 March 2012

Abstract

Laminated SiC/ZrB_2 ceramic was fabricated by roll-compaction and spark plasma sintering at 1600 °C. A maximum fracture toughness of 12.3 ± 0.3 MPa $m^{1/2}$ was measured for the sintered SiC/ZrB_2 laminated ceramic. This significant improvement in fracture toughness can be attributed to the crack deflection along the interfacial layer and the presence of residual stresses in the sample. The effect of interlayer composition on the residual stresses was discussed in detail. It is observed that the residual thermal stress could be reduced by addition of ZrB_2 particles to the SiC interlayer. The bending strength can be increased to 388 ± 44 MPa with the addition of 20 vol% ZrB_2 to the SiC interlayer.

Keywords: C. Mechanical properties; Laminated composites; Zirconium diboride; Spark plasma sintering

1. Introduction

Zirconium diboride (ZrB_2) is one of the most promising ceramic for ultra-high temperature applications because of its higher melting temperature (>3000 °C), excellent strength at elevated temperatures, and high thermal conductivity [1]. Silicon carbide (SiC) is commonly added to ZrB_2 to improve its oxidation resistance, mechanical strength, fracture toughness, and sintering behavior [2–5]. Therefore, a lot of research has been carried out on SiC/ZrB_2 composites as it is a potential candidate material for use in thermal protection systems and hypersonic flight vehicles. However, the actual uses of ZrB_2-based ceramics are limited due to its low fracture toughness. Hence particle or whisker reinforcements are commonly used to improve the toughness and the resistance to damage of ZrB_2-based ceramics. The fracture toughness of ZrB_2 ceramics with particle reinforcements was reportedly in the range of 2.4–4.8 MPa $m^{1/2}$ [6–9], which could be further increased to 6.11–8.08 MPa $m^{1/2}$ with the addition of the second phase with a higher aspect ratio (e.g., flakes or rods/whiskers) [10–14]. Recently, a toughness of 6.7 MPa $m^{1/2}$ was reached in ZrB_2–ZrC–SiC system by controlling microstructure through an in situ synthesis processing method [15,16]. The advantages of elongated secondary phases are crack deflection, crack bridging and pullout. However, most of the toughening effects may diminish with increasing temperature.

One of the most promising new approaches is to improve toughness of ceramics through preparation of laminated materials [17]. In the past decade, laminated ceramics, usually consisting of strong matrix layers and weaker interlayer arranged alternately, have been extensively studied to make high-toughness ceramics, such as SiC/TiB_2, Al_2O_3/ZrO_2 and Si_3N_4/BN laminated ceramic composites [18–22]. Such laminated structure endows the ceramic composites high toughness, energy absorption and/or non-catastrophic failure behavior. Huang and Wang have fabricated planar laminates with apparent fracture toughness as high as 15.1 MPa $m^{1/2}$ by controlling composition and structure of Si_3N_4/BN laminates [23]. Even higher fracture toughness of 28.1 MPa $m^{1/2}$ was obtained by adding secondary reinforcement such as SiC whiskers to the BN interface [24]. Due to the excellent advantages of laminated structures, some researchers have

* Corresponding author.
E-mail address: 119whl@zzu.edu.cn (H. Wang).

0272-8842/$36.00
doi:10.1016/j.ceramint.2012.02.098

made great efforts to fabricate ZrB_2-based laminated composites to improve the fracture toughness of ZrB_2-based ceramics [25]. In the case of layered ceramics, there are two main methods used to enhance toughness over conventional ceramics, namely introducing low energy paths for crack propagation or making the presence of residual stresses. Recently, some research has been reported on the toughening of laminated ZrB_2-SiC with residual stresses [26–28]. In our previous works, we also prepared ZrB_2/Mo and ZrB_2/SiC laminate composites with a relative high fracture toughness [29,30]. Nevertheless, hot pressing (HP) has been used as a major fabrication technique for laminates. In case of HP, the total sintering time is more than 4 h, which induces grain growth. On the other hand, spark plasma sintering (SPS) is one of the most advanced processing techniques to obtain dense ceramics at low sintering temperature. The mechanisms and phenomena on which SPS is based are not completely clarified. However, a pulse current passing through the processing powders is supposed to generate a plasma discharge within the voids among particles. High-energy plasma sintering can cause particle surface activation, local melting, and evaporation on the surface of the powders, which induce neck formation between particles. The SPS process makes it possible to sinter diboride based ceramics (ZrB_2, HfB_2, and TiB_2) at a lower temperature and in a shorter time compared with the conventional techniques such as HP [31–34].

The main objective of present study is to explore the possibility to obtain laminated SiC/ZrB_2 ceramic with high toughness by spark plasma sintering. Here we used spark plasma sintering instead of hot pressing since sintering is fast due to fast heating/cooling rate and lower sintering temperature with SPS. The extremely rapid cooling rate during SPS may cause larger residual stresses, which contribute to toughen ZrB_2 matrix ceramic. Laminated SiC/ZrB_2 ceramic was fabricated by roll-compaction and spark plasma sintering. The microstructure and mechanical properties, such as flexure strength and fracture toughness and work of fracture were evaluated to understand the laminated structure and composites on mechanical behavior. The effect of interlayer composition on the residual stress was discussed in detail.

Table 1
The bending strength and fracture toughness of the SiC/ZrB_2 laminated composites prepared by spark plasma sintering.

Samples	Composition of the interlayers	Bending strength (MPa)	Fracture toughness (MPa $m^{1/2}$)
ZSSPS1	SiC	216 ± 75	6.1 ± 0.3
ZSSPS2	SiC + 10%ZrB_2	117 ± 98	6.9 ± 0.2
ZSSPS3	SiC + 20%ZrB_2	388 ± 44	9.9 ± 0.4
ZSSPS4	SiC + 30%ZrB_2	379 ± 64	12.3 ± 0.3
ZSSPS5	SiC + 50%ZrB_2	277 ± 26	7.8 ± 0.8

2. Experimental procedures

Commercially available ZrB_2 (purity ~95% with ZrO_2 as main impurity, mean particle size ~6.7 μm), nano-SiC whiskers (β-type, 99.5% pure, mean diameter < 100 nm, aspect ratio > 10) and SiC powders (99.9% pure, mean diameter < 1 μm) were used in this work. In the ZrB_2 matrix layers, 10 vol% SiC whiskers and 10 vol% SiC particles were added to reinforce the matrix layers. The composition of the interlayer was the SiC powers with various volume fractions of ZrB_2 (0–50%) particles. The composition and the properties of the interlayer are listed in Table 1.

The fabrication process of SiC/ZrB_2 laminated ceramics is schematically illustrated in Fig. 1. Nano-SiC whiskers and SiC particles were dispersed for 15 min in ethanol by an ultrasonic device and then mixed with ZrB_2 powders in ethanol by ball-milling for 4 h. After drying, the powder mixture was blended with 10 wt% organic polymer binders (PVA) and 1 wt% plasticizing agent (glycerin) by roll-compaction. After repeated rolling, thin sheets of ~0.2 mm thick was formed. Subse-

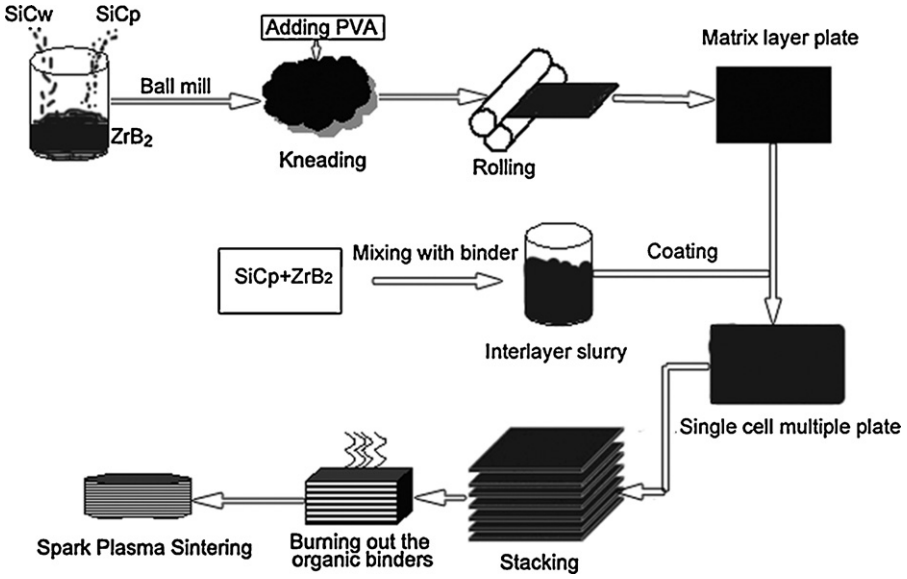

Fig. 1. Flow chart for fabrication of the SiC/ZrB_2 laminated ceramics.

quently, the sheets were dried and cut into circular shape with a diameter of ~30 mm, which were the matrix layers. The circular sheets were then dip-coated with SiC slurry containing 0–50 vol% ZrB_2. After drying, the coated sheets were stacked in a graphite die and heated slowly to 500 °C in order to remove the organic binders. Afterwards, the green bodies were sintered by SPS at 1600 °C for 5 min under vacuum conditions (<6 Pa) with an SPS-510L apparatus (Sumitomo Coal Mining, Tokyo, Japan). A pressure of 40 MPa and an on-off pulse sequence of 12:2 were applied to the sample during the sintering process. The temperature of the specimen was measured through the side hole of the graphite mold with an optical pyrometer (Chino IR-AHS, Japan). The processing parameters (temperature, *z*-displacement, pressure) were recorded every 30 s.

Sintered samples were cut and ground into test bars with a dimension of 3 mm × 2 mm × 25 mm. The thickness direction of the specimens was perpendicular to the layers. Each bar was polished with diamond pastes down to 1 μm on the side, which was vertical to the pressing direction. The two edges near the tensile surface were rounded with a 15 mm diamond grinding wheel. The mechanical properties of the samples were determined with a mechanical test machine (Astron AG2000A). The strength measurement was carried out using a three-point bending method with a span of 10 mm and a crosshead speed of 0.5 mm/min. The fracture toughness was measured using the single edge notched beam (SENB) method. The dimension of the test bars was 4 mm × 2 mm × 28 mm. The testing was conducted with a crosshead speed of 0.05 mm/min and a span of 24 mm. The tensile surface of the samples was parallel to the stacking direction. A minimum of 5 specimens were tested for each experimental condition.

The polished surface parallel to the pressing direction, the fracture structure and the crack propagating paths were examined with a scanning electron microscopy (SEM, JEOL JSM-6700F, Tokyo).

3. Results and discussion

3.1. Layers microstructure

Fig. 2(a) shows SEM micrographs of the side surface of the ZSSPS1 sample, in which the dark layers were the SiC interlayers, and the gray layers were the ZrB_2 matrix layers. The thickness of each matrix layer was about 100 μm, but the thickness of each SiC interlayer was not uniform. These non-uniform structures indicate that the SiC interlayer was not fully sintered. However, the structure of the interlayer was modulated by the adding ZrB_2 particles. The characteristic structures of the sample with 30 vol% ZrB_2 particles in the interlayers are shown in Fig. 2(b). It can be found that the thickness of the interlayer became thinner and uniform. This means the additions of ZrB_2 particles can promote the densification behavior of the SiC interlayer. The enhanced sintering at lower temperature is due to the liquid phase formation by the reaction between the oxides present on the surface of the ZrB_2 and the SiC particles.

3.2. Fracture toughness and failure behavior

The fracture toughness of the SiC/ZrB_2 laminated composite prepared by spark plasma sintering is shown in Table 1. The fracture toughness of the SiC/ZrB_2 laminated composites was various for the components of the interlayer changed, which increased to 12.3 ± 0.3 MPa $m^{1/2}$ on the addition of 30 vol% ZrB_2 particle to the SiC interlayer. It is widely recognized that the critical notch root radius can have a large impact on the measured toughness value. To obtain valid results, it is necessary to cut suitably thin notches [35]. In the present investigation, the critical notch root radius was determined to be about 100 μm and the narrowest notch width was about 250 μm, which were large than the reference material [36]. Therefore, only comparing with the toughness values of several ZrB_2-based materials produced in our labs, the toughness of SiC/ZrB_2 laminated ceramic was twice higher than the value for the ZrB_2 monolithic ceramics [37]. In order to elucidate the toughening mechanisms, the propagation path of the cracks in the SiC/ZrB_2 laminated ceramics are observed by SEM (shown in Fig. 3). As shown in Fig. 3(a), a major crack still propagated through the specimen although it was lightly deflected by the interlayer. One remarkable feature observed in Fig. 3(b), (c) and (d) was the delaminating crack along the interface layers, which could act more effectively as an energy-absorbing mechanism and toughen the material further. The delaminating crack was due to the presence of compressive residual stresses within the

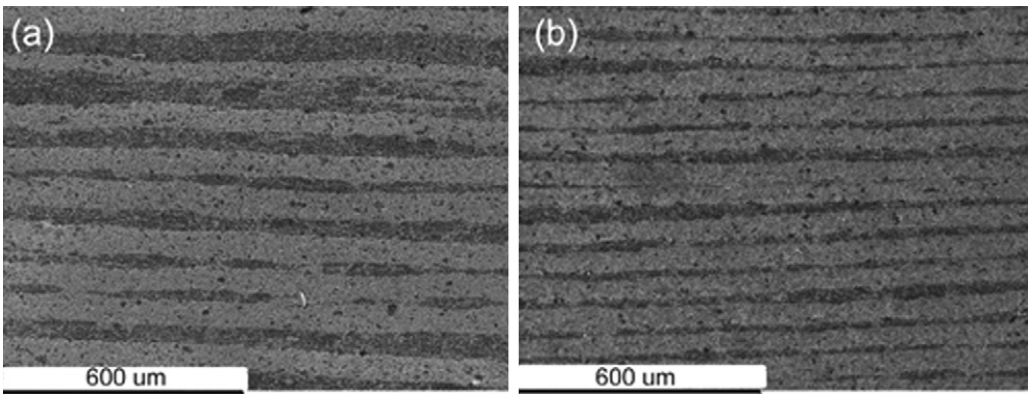

Fig. 2. Morphology of the SiC/ZrB_2 laminated composites: (a) ZSSPS1 and (b) ZSSPS4.

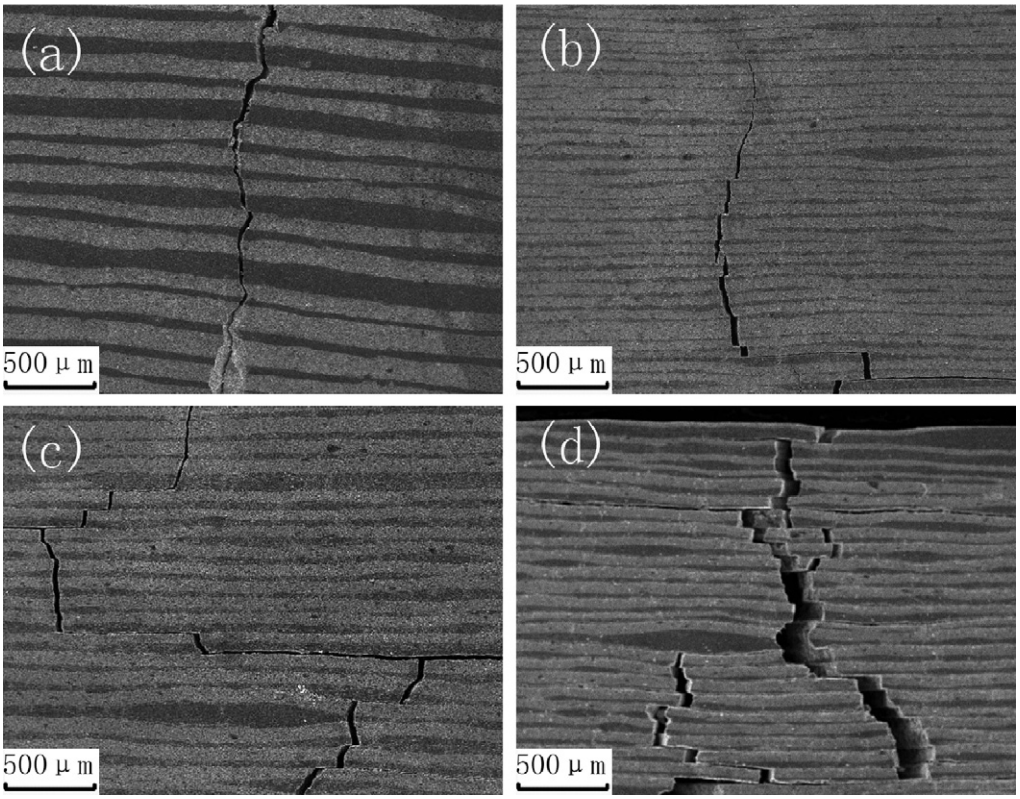

Fig. 3. The crack propagation in SiC/ZrB_2 laminated composites: (a) ZSSPS1, (b) ZSSPS3, (c) ZSSPS4 and (d) ZSSPS5.

interface layers, which acted as a barrier to crack propagation [38]. Fig. 4 presents the typical load–displacement curves of the SiC/ZrB_2 laminated composites. It can be seen that the laminated ceramic showed a plastic-like characteristic in the load–displacement curve. This behavior has been observed by other authors in other laminated structures [39]. As it can be inferred from Fig. 4(b), the first slope change in the load–displacement curve seen may be related to cracking of the matrix layer at the bottom of the notch. After the crack growth passed through one or two of the matrix layers, it might be arrested by the compressive residual stresses within the interface layer, then propagated parallel to the layers which induced a change in the stress state, leading to the following load extends at the load–displacement curve [36,40,41]. The sample had many remainder perfect matrix layers which could support the continuous applied load and the same amount of compressive interface layers which acted as a barrier to crack propagation. Then the load-bearing ability of this sample decreased with the amount of integrated layers decreasing. The work of fracture of each specimen was calculated by determining the area under the load-crosshead deflection curve and dividing it by twice the cross-sectional area of the sample. As the displacement further increased, the work of fracture of these laminated composites was higher than the monolithic ceramic. The apparent work of fracture for the ZSSPS3 and ZSSPS4 samples were 2371 J/m^2 and 2140 J/m^2, respectively. Thus, laminated ceramics showed a non-catastrophic failure. The main reason for such high work of fracture might be related to the presence of the compressive interface layers, which act as a barrier against any possible crack propagation. Forevermore, the compressive layers can lead to the crack deflection and bifurcation, as shown in Fig. 3(d). This phenomenon might increase the energy absorption capability of the material [17,42,43].

3.3. Bending strength and residual stress

As shown in Table 1, most of the bending strength of the SiC/ZrB_2 laminated composites was lower than that of monolithic ZrB_2 ceramic produced in our labs [44]. The highest bending strength was 388 ± 44 MPa, which was the same level as the strength of a monolithic ZrB_2 ceramic. The decrease in bending strength is related to the densification behavior of the laminated composites and the tensile residual stresses in the materials. As shown in Fig. 5(a), the SiC interlayer of the ZSSPS1 sample was not fully densed. There were holes and defects in the interlayer. Furthermore, there was obvious crack in the middle of the interlayer, where was the bonding region of the two sheets during stacking processing. This indicated that the bonding strength of each interface layers was poor, and the laminated materials could be delaminated easily parallel the interlayer. This failure mode occurred once in a while during the fabrication of the laminated materials, shown in Fig. 5(b). All the above phenomena could reduce the strength of the laminated materials and then the bending strength of the ZSSPS1 sample was lower than that of the monolithic ZrB_2.

The densification behavior of the SiC interlayer can be increased by the addition of ZrB_2 particles. Firstly, during the SPS, a pulsed direct electric current passed through the graphite die, depending on the electrical conductivity of the material to

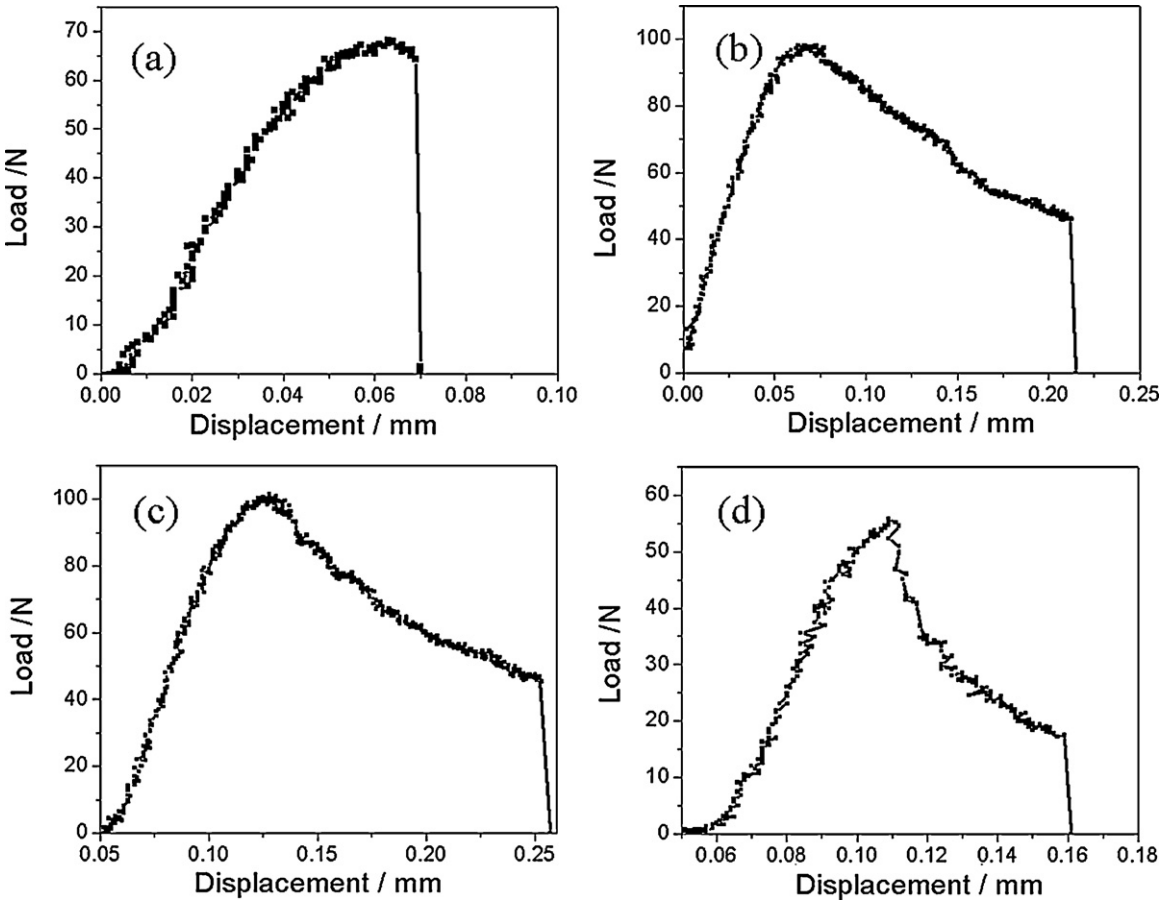

Fig. 4. Typical load–displacement curves of the SiC/ZrB_2 laminated composites: (a) ZSSPS1, (b) ZSSPS3, (c) ZSSPS4 and (d) ZSSPS5.

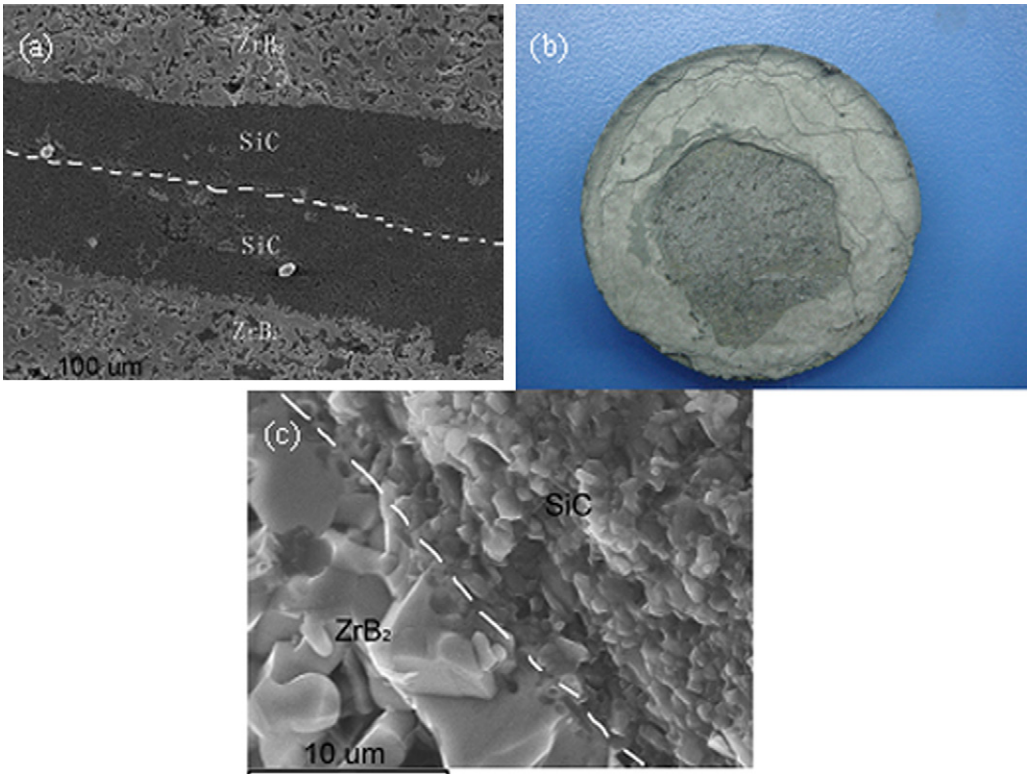

Fig. 5. Microstructures of the SiC/ZrB_2 laminated composites: (a) the ZSSPS1 sample, (c) the ZSSPS3 sample and photo of the ZSSPS1 sample damaged during the fabrication (b).

be sintered. ZrB_2 has a high electrical conductivity, which could improve electrical current propagation through the SiC interlayer, resulting in a current-activated sintering. Secondly, the oxide existing on the surface of the ZrB_2 particles and the SiC particles could react with each other, forming glass phase through eutectic reaction, which contribute to improve the densification behavior of the SiC interlayer. The microstructure of the ZSSPS3 sample is shown in Fig. 5(c). It could be found that the structure of the ZSSPS3 sample was denser than that of the ZSSPS1 sample. The grain size of the ZrB_2 and the SiC was same as that of the raw materials (see Section 2). There were fewer voids in the interlayer than those in the ZSSPS1 sample, and there were also few defects between the interlayer and the matrix layer. Moreover, the residual stresses in the laminated materials could be reduced by the ZrB_2 particles adding to the SiC interlayer. In case of unmatched thermal expansion coefficients of the matrix layers and interlayer, internal residual stress would be introduced into the laminated composites on cooling from sintering temperature to ambient temperature. This should be in favor of increasing the toughness of the composites as discussed before. However, the reliability multilayer composite should have the highest compressive stresses in the internal layers with the lowest tensile ones at the surface based on a residual stress view point [45–47]. A high tensile residual stress would produce the formation of the observed micro cracks. Then the laminate design was done taking into account the total strain of monolithic materials of both compositions when cooling from the highest sintering temperature and their elastic modulus in order to limit tensile residual stresses in the external layers. In accordance with the principles of composite, the difference of the CTE and elastic modulus of each layers could be reduced by composites designed.

$$E_c = \frac{1}{2}\left(E_{SiC}V_{SiC} + E_{ZrB_2}V_{ZrB_2} + \left(\frac{1}{V_{SiC}/E_{SiC} + V_{ZrB_2}/E_{ZrB_2}}\right)\right) \quad (1)$$

The elastic modulus and CTEs of the layers composited with SiC and ZrB_2 components are given by:

$$\alpha_c = \alpha_{SiC}V_{SiC} + \alpha_{ZrB_2}V_{ZrB_2} \quad (2)$$

where E_c, E_{SiC} and E_{ZrB_2} are the elastic modulus of the layer composite, SiC phase and ZrB_2 phase, respectively. V_{SiC} and V_{ZrB_2} are the volume fraction of the SiC phase and ZrB_2 phase. α_c, α_{SiC} and α_{ZrB_2} are the thermal expansion coefficient of the composite, SiC phase and ZrB_2 phase, respectively.

Table 2 shows the CTE, Poisson's ratio and elastic modulus of SiC, ZrB_2, and the layer composites of each laminated composites [48,49]. It can be found that the difference of the CTE between SiC and ZrB_2 was large, and that could be reduced by modulation of each layer composites. Chartier [50] has proposed a simple formula to calculate the residual stress for a multilayered system composed n layers of composite X and thickness d_x and $n-1$ layers of composition Y and thickness d_y. And the residual stresses values in the bulk of each layer may be estimated as:

Table 2
CTEs, Poisson's ratio and elastic modulus of materials in laminated ceramics.

Materials	Elastic modulus (GPa)	Poisson's ratio	CTE ($\times 10^{-6}$ K^{-1})
ZrB_2	490	0.17	6.7
SiC	550	0.14	4.7
The matrix layer	501.5	0.164	6.3
The interface layer			
ZSSPS1	550	0.14	4.7
ZSSPS2	543.7	0.143	4.9
ZSSPS3	537.4	0.146	5.1
ZSSPS4	531.3	0.149	5.3
ZSSPS5	519.1	0.155	5.7

$$\sigma_x = \frac{(n-1)E_xE_yd_y\,\Delta\alpha\,\Delta T}{(n-1)(1-\upsilon_x)E_yd_y + n(1-\upsilon_y)E_xd_x} \quad (3)$$

$$\sigma_y = -\frac{nE_xE_yd_x\,\Delta\alpha\,\Delta T}{(n-1)(1-\upsilon_x)E_yd_y + n(1-\upsilon_y)E_xd_x} \quad (4)$$

where E_i and υ_i ($i = x, y$) are the elastic modulus and Poisson's ratio of each layer. $\Delta\alpha$ is difference of the thermal expansion coefficient of each layer. The value of ΔT is calculated from sintering temperature to room temperature, namely, 1600–25 °C = 1575 °C. According to formula, the value and distribution of the tensile stress and compressive stress are shown in Table 3.

Upon analysis of the stress in the laminated composites, materials with large mismatch of thermal expansion between layers (the ZSSPS1 sample) had a high tensile residual stress within the matrix layers at 261 MPa. As the matrix layers were out layer, the tensile stress would decrease the strength of the laminated composites. So the ZSSPS1 sample has a low strength and sometimes should be damaged by this residual stress, as shown in Fig. 5(b). However, the residual stress in the laminated composites decreased with the thermal expansion mismatch between layers decreasing. Even if the compressive stress within the interface layers decreased at the same time, that still kept a high value at −485 MPa in the ZSSPS5 sample. Therefore, the ZSSPS3 sample showed a high fracture toughness and good strength as the high compressive stresses in the interface layers and the low tensile ones at the matrix layers.

Table 3
Residual stress in the SiC/ZrB_2 laminated composites.

Sample	Tensile stress in the matrix layers (MPa)	Compressive stress in the interlayer (MPa)
ZSSPS1	261	−1331
ZSSPS2	227	−1158
ZSSPS3	193	−984
ZSSPS4	160	−816
ZSSPS5	95	−485

4. Conclusions

The SiC/ZrB_2 composites with laminated structure have been successfully prepared by spark plasma sintering at 1600 °C. The maximum apparent fracture toughness of these laminated SiC/ZrB_2 composites was 12.3 ± 0.3 MPa $m^{1/2}$, respectively. The load–displacement curve of the material appears nonlinear and this material shows a non-catastrophic failure. The flexural strength of the specimens was affected by the residual porosity and the residual thermal stress state. The maximum bending strength of these specimens was 388 ± 44 MPa. The theoretical calculations indicated that the addition of the ZrB_2 particle to the SiC interlayer was in favor of decreasing the tensile stress in surface layer and improving the sintering behavior and strength of the laminated composites. It appeared that the enhancement of the fracture energy for the laminated composite was mainly attributed to the delaminating crack and crack deflection, due to the high compressive stress state. These results showed that the laminated composites with the high compressive stresses in the interface layers and the low tensile stress at the matrix layers were possible to produce highly reliable ceramic materials in ultra-high temperature application.

Acknowledgements

This work was financial support from the 973 program from Ministry of Science and Technology of China (grant no. 5133102-4), the National Natural Science Foundation of China (no. 51002142). State Key Laboratory of New Ceramic and Fine Processing, Tsinghua University (KF09010) and China Postdoctoral Science Foundation (grant no.: 20100471001) funded project are greatly appreciated.

References

[1] S.Q. Guo, Densification of ZrB_2-based composites and their mechanical and physical properties: a review, J. Eur. Ceram. Soc. 29 (2009) 995–1011.
[2] Z. Wu, Z. Wang, G. Shi, J. Sheng, Effect of surface oxidation on thermal shock resistance of the ZrB_2–SiC–ZrC ceramic, Compos. Sci. Technol. 71 (2011) 1501–1506.
[3] J. Zou, S.K. Sun, G.J. Zhang, Y.M. Kan, P.L. Wang, T. Ohji, Chemical reactions, anisotropic grain growth and sintering mechanisms of self-reinforced ZrB_2–SiC doped with WC, J. Am. Ceram. Soc. 94 (2011) 1575–1583.
[4] V. Medri, C. Capiani, A. Bellosi, Properties of slip-cast and pressureless-sintered ZrB_2–SiC composites, Int. J. Appl. Ceram. Technol. 83 (2011) 51–359.
[5] L. Rangaraj, C. Divakar, V. Jayaram, Fabrication and mechanisms of densification of ZrB_2-based ultra high temperature ceramics by reactive hot pressing, J. Eur. Ceram. Soc. 30 (2010) 129–138.
[6] F. Monteverde, S. Guicciardi, A. Bellosi, Advances in microstructure and mechanical properties of zirconium diboride based ceramics, Mater. Sci. Eng. A346 (2003) 310–319.
[7] A.L. Chamberlain, W.G. Fahrenholtz, G.E. Hilmas, D.T. Ellerby, High-strength zirconium diboride-based ceramics, J. Am. Ceram. Soc. 87 (2004) 1170–1172.
[8] A. Rezaie, W.G. Fahrenholtz, G.E. Hilmas, Effect of hot pressing time and temperature on the microstructure and mechanical properties of ZrB_2–SiC, J. Mater. Sci. 42 (2007) 2735–2744.
[9] J.K. Kurihara, T. Tomimatsu, Y.F. Liu, S.Q. Guo, Y. Kagawa, Mode I fracture toughness of SiC particle-dispersed ZrB_2 matrix composite measured using DCDC specimen, Ceram. Int. 36 (2010) 381–384.
[10] S. Zhou, Z. Wang, X. Sun, J. Han, Microstructure, mechanical properties and thermal shock resistance of zirconium diboride containing silicon carbide ceramic toughened by carbon black, Mater. Chem. Phys. 122 (2010) 470–473.
[11] H. Chen, Z. Wang, S. Meng, G. Bai, W. Qu, The failure mechanism of ZrB_2–SiC–graphite composite heated by high electric current, Mater. Lett. 63 (2009) 2346–2348.
[12] S.Q. Guo, Y. Kagawa, T. Nishimura, D. Chung, J.-M. Yang, Mechanical and physical behavior of spark plasma sintered ZrC–ZrB_2–SiC composites, J. Eur. Ceram. Soc. 28 (2008) 1279–1285.
[13] X.H. Zhang, L. Xu, W.B. Han, L. Weng, J.C. Han, S.Y. Du, Microstructure and properties of silicon carbide whisker reinforced zirconium diboride ultra-high temperature ceramics, Solid State Sci. 11 (2009) 156–161.
[14] Y. Wang, M. Zhu, L. Cheng, L. Zhang, Fabrication of SiCw reinforced ZrB_2-based ceramics, Ceram. Int. 36 (2010) 1787–1790.
[15] Q. Qu, J.C. Han, W.B. Han, X.H. Zhang, C.Q. Hong, In situ synthesis mechanism and characterization of ZrB_2–ZrC–SiC ultra high-temperature ceramics, Mater. Chem. Phys. 110 (2008) 216–221.
[16] D. Sciti, L. Silvestroni, V. Medri, S. Guicciardi, Pressureless sintered in situ toughened ZrB_2–SiC platelets ceramics, J. Eur. Ceram. Soc. 31 (2011) 2145–2153.
[17] W.J. Clegg, K. Kendall, N.M. Alford, T.W. Button, J.D. Birchall, A simple way to make tough ceramics, Nature 347 (1990) 455–457.
[18] D. Kovar, M.D. Thouless, J.W. Halloran, Crack deflection and propagation in layered silicon nitride/boron nitride ceramics, J. Am. Ceram. Soc. 81 (1998) 1004–1012.
[19] H. Tomaszewski, H. Weglarz, A. Wajler, M. Boniecki, D. Kalinski, Multilayer ceramic composites with high failure resistance, J. Eur. Ceram. Soc. 27 (2007) 1373–1377.
[20] R. Bermejo, R. Danzer, High failure resistance layered ceramics using crack bifurcation and interface delamination as reinforcement mechanisms, Eng. Fract. Mech. 77 (2010) 2126–2135.
[21] O.N. Grigoriev, A.V. Karoteev, E.N. Maiboroda, I.L. Berezhinsky, B.K. Serdega, D.Yu. Ostrovoi, V.G. Piskunov, Structure, nonlinear stress–strain state and strength of ceramic multilayered composites, Composites B37 (2006) 30–541.
[22] Z. Krstic, V.D. Krstic, Fracture toughness of concentric Si_3N_4-based laminated structures, J. Eur. Ceram. Soc. 29 (2009) 1825–1829.
[23] Y. Huang, S.K. Zhao, C.W. Li, C.A. Wang, Q.F. Zang, Flexure creep behaviors of Si_3N_4/BN laminated ceramic composites produced by rolling, Key Eng. Mater. 249 (2003) 15–24.
[24] C.A. Wang, Y. Huang, Q.F. Zan, L.H. Zou, S.Y. Cai, Control of composition and structure in laminated silicon nitride/boron nitride composites, J. Am. Ceram. Soc. 85 (2002) 2457–2461.
[25] P. Zhou, P. Hu, X. Zhang, W. Han, Laminated ZrB_2–SiC ceramic with improved strength and toughness, Scr. Mater. 64 (2011) 276–279.
[26] X. Zhang, P. Zhou, P. Hu, W. Han, Toughening of laminated ZrB_2–SiC ceramics with residual surface compression, J. Eur. Ceram. Soc. 31 (2011) 2415–2423.
[27] Z. Lü, D. Jiang, J. Zhang, Q. Lin, Z. Huang, ZrB_2–SiC laminated ceramic composites, J. Eur. Ceram. Soc. doi:10.1016/j.jeurceramsoc.2011.04.020, in press.
[28] V. Medri, P. Pinasco, A. Sanson, E. Roncari, S. Guicciardi, A. Bellosi, ZrB_2-based laminates produced by tape casting, Int. J. Appl. Ceram. Technol. doi:10.1111/j.1744-7402.2011.02630.x, in press.
[29] H. Wang, C.A. Wang, R. Zhang, X. Hu, Y. Huang, Preparation and mechanical properties of ZrB_2-based laminated composites, Rare Metal. Mater. Eng. 36 (2007) 841–843.
[30] C.A. Wang, H.L. Wang, L. Yu, Y. Huang, Microstructure and mechanical properties of ZrB_2-based composites with laminated structure, Int. J. Mater. Product Technol. 37 (2010) 228–232.
[31] T. Mizuguchi, S. Guo, Y. Kagawa, Transmission electron microscopy characterization of spark plasma sintered ZrB_2 ceramic, Ceram. Int. 36 (2010) 943–946.

[32] V.M. Sglavo, F.D. Genua, A. Molinari, Alumina/silicon carbide laminated composites by spark plasma sintering, J. Am. Ceram. Soc. 92 (2009) 2693–2697.
[33] Y. Zhao, L.J. Wang, G.J. Zhang, W. Jiang, L.D. Chen, Preparation and microstructure of a ZrB_2–SiC composite fabricated by the spark plasma sintering-reactive synthesis (SPS-RS) method, J. Am. Ceram. Soc. 90 (2007) 4040–4042.
[34] A. Bellosi, F. Monteverde, D. Sciti, Fast densification of ultra-high-temperature ceramics by spark plasma sintering, Int. J. Appl. Ceram. Technol. 3 (2006) 32–40.
[35] R. Damani, R. Gstrein, R. Danzer, Critical notch-root radius effect in SENB-S fracture toughness testing, J. Eur. Ceram. Soc. 16 (1996) 695–702.
[36] R. Bermejo, Y. Torres, M. Anglada, L. Llanes, Fatigue behavior of alumina–zirconia multilayered ceramics, J. Am. Ceram. Soc. 91 (2008) 1618–1625.
[37] H.L. Wang, C.A. Wang, X.F. Yao, D.N. Fang, Processing and mechanical properties of zirconium diboride-based ceramics prepared by spark plasma sintering, J. Am. Ceram. Soc. 90 (2007) 1992–1997.
[38] R. Bermejo, A.J. Sanchez-Herencia, L. Llanes, C. Baudin, High-temperature mechanical behaviour of flaw tolerant alumina–zirconia multilayered ceramics, Acta Mater. 55 (2007) 4891–4901.
[39] C. Li, Y. Huang, C.A. Wang, K. Tang, S. Li, Q. Zan, Mechanical properties and microstructure of laminated Si_3N_4 + SiCw/BN + Al_2O_3 ceramics densified by spark plasma sintering, Mater. Lett. 57 (2002) 336–342.
[40] R. Bermejo, Y. Torres, C. Baudín, A.J. Sánchez-Herencia, J. Pascual, M. Anglada, L. Llanes, Threshold strength evaluation on an Al_2O_3–ZrO_2 multilayered system, J. Eur. Ceram. Soc. 27 (2007) 1443–1448.
[41] V.M. Sglavo, M. Bertoldi, Design and production of ceramic laminates with high mechanical resistance and reliability, Acta Mater. 54 (2006) 4929–4937.
[42] A.J. Sánchez-Herencia, C. Pascual, J. He, F.F. Lange, ZrO_2/ZrO_2 layered composites for crack bifurcation, J. Am. Ceram. Soc. 82 (1999) 1512–1518.
[43] M.G. Pontin, F.F. Lange, Crack bifurcation at the surface of laminar ceramics that exhibit a threshold strength, J. Am. Ceram. Soc. 88 (2005) 1315–1317.
[44] C.A. Wang, H. Wang, Y. Huang, D. Fang, Preparation and flame ablation/oxidation behavior of ZrB_2/SiC ultra-high temperature ceramic composites, Key Eng. Mater. 351 (2007) 142–146.
[45] R. Bermejo, Y. Torres, A.J. Sánchez-Herencia, C. Baudín, M. Anglada, L. Llanes, Residual stresses, strength and toughness of laminates with different layer thickness ratios, Acta Mater. 54 (2006) 4745–4757.
[46] C.R. Chen, R. Bermejo, O. Kolednik, Numerical analysis on special cracking phenomena of residual compressive inter-layers in ceramic laminates, Eng. Fract. Mech. 77 (2010) 567–2576.
[47] L. Sestakova, R. Bermejo, Z. Chlup, R. Danzer, Strategies for fracture toughness, strength and reliability optimisation of ceramic–ceramic laminates, Int. J. Mat. Res. 102 (2011) 613–626.
[48] C. Wei, X. Zhang, P. Hu, W. Han, S. Li, Microstructure and mechanical properties of laminated ZrB_2–SiC ceramics with ZrO_2 interface layers, Int. J. Refract. Met. Hard Mater. 30 (2012) 173–176.
[49] Z. Wang, S. Wang, X.H. Zhang, P. Hu, W.B. Han, C.Q. Hong, Effect of graphite flake on microstructure as well as mechanical properties and thermal shock resistance of ZrB_2–SiC matrix ultrahigh temperature ceramics, J. Alloys Compd. 484 (2009) 390–394.
[50] T. Chartier, D. Merle, J. Besson, Laminar ceramic composites, J. Eur. Ceram. Soc. 15 (1995) 101–107.